Preliminary Studies for Obtaining Ac-225 by Irradiating Ra-266 Inorganic Compounds with Proton Beams

H. Barcellos e I. P. Miranda
Instituto de Pesquisas Energéticas e Nucleares
Av. Prof. Lineu Prestes, 2242
05508-000 – São Paulo, SP
hbolivei@ipen.br

Abstract

Targeted Alpha Therapy uses radionuclides that emit alpha particles, which, due to their short physical range, minimize damage to surrounding tissues. Actinium-225 stands out in this type of therapy, especially when conventional treatments are ineffective.This work aims to obtain quantitative data, through numerical simulations using the Monte Carlo method, for the production of ^{225}Ac by irradiation of inorganic ^{226}Ra compounds with low- to medium-energy proton beams. Six distinct targets were evaluated: purified ^{226}Ra in metallic form, $RaCl_2$, RaO, $Ra(OH)_2$, $RaCO_3$, and $Ra(NO_3)_2$. Simulated irradiations were performed using 30 MeV proton beams for 45 hours at a beam current of 50 μA. The ^{225}Ac activities produced were measured at four time points: at the end of irradiation (EOB) and at 20, 50, and 100 days after EOB. The results showed that the practical yield of ^{225}Ac production ranged from 1.70 MBq/μAh for the metallic ^{226}Ra target to 0.70 MBq/μAh for the radium nitrate target.

1. Introduction

Targeted alpha therapy is a developing technique that uses alpha-emitting radionuclides combined with selective delivery vectors (peptides, antibodies, nanoparticles). These alpha-emitters deliver highly localized, intense radiation to cancer cells, thereby reducing damage to surrounding healthy cells. This is due to the short distance traveled by the alpha-emitter and the high linear energy transfer, which allows for greater precision [1,2].

Actinidium-225 is an alpha-emitting radionuclide that has attracted considerable attention in Nuclear Medicine with applications in cancer treatments. The potential of radiopharmaceuticals labeled with this radionuclide in cancer treatment lies in their ability to induce DNA double-strand breaks, thereby inhibiting cell proliferation. ^{225}Ac generates eight short-lived decay products (^{221}Fr, ^{217}At, ^{213}Bi, ^{213}Po, ^{209}Pb, and stable ^{209}Bi), emitting four alpha particles in this decay chain, ultimately yielding a lethal dose to cancer cells [3]. It is important to note that ^{225}Ac therapy has proven effective, particularly in patients who have not responded to other cancer treatments [4,5]. Despite some promising clinical results, significant research is still needed to optimize the implementation of targeted alpha therapy.Currently, there are several investigational production routes for ^{225}Ac; however, the main clinical source of ^{225}Ac is derived from ^{232}Th stock. ^{225}Ac is isolated using a generator system and supplied with high specific activity. Recently, the US Department of Energy has been producing ^{225}Ac regularly by spallation of ^{232}Th with high-energy protons (100 MeV or more) [4,7,8].

There is the possibility of generating clinically significant quantities of ^{225}Ac by irradiating ^{226}Ra compounds (T1/2 = 1600 y) with low- and medium-energy protons or photons [9,10,11,12]. The main challenges with radio compound targets are handling and availability. 226Ra contains several daughter radionuclides, with ^{222}Rn (T1/2 = 3.8 d) being an inert, radioactive gas that can hinder target design, handling, and subsequent radiochemistry. Although no products from ^{226}Ra are currently available, several research centers and commercial companies have studied this possibility over the past 10 years.

Therefore, the main objective of this work is to obtain relevant data via Monte Carlo simulations to model the production of ^{225}Ac by irradiating ^{226}Ra compounds with low- and medium-energy proton beams.

2. Methodology

For the elaboration of this work, the first step was to determine the proton-beam energy that would produce the highest ^{225}Ac activity. Six different inorganic compounds of ^{226}Ra were chosen, namely: purified ^{226}Ra in metallic form; radium chloride ($RaCl_2$); radium carbonate ($RaCO_3$); radium nitrate ($Ra(NO_3)_2$); radium hydroxide ($Ra(OH)_2$); and radium oxide (RaO). All targets have the same dimensions: 0.5 cm radius and 100 µm thickness, deposited on an aluminum substrate with a diameter of 0.7 cm and a thickness of 0.25 cm. Figure 1 illustrates the geometry used in the simulations.

Based on data provided by the Nuclear Energy Agency (NEA)[13], the peak cross-section for ^{225}Ac production by irradiating ^{226}Ra targets with protons is in the range between 14 and 16 MeV, as shown in Figure 2. Thus, simulated irradiations were performed with energies between 13 MeV and 17 MeV (+/- 0.05 MeV) in 1.0 MeV intervals. The irradiation time was 40 h with a beam current of 50 µA. Figure 3 shows the graphs of the ^{225}Ac produced activities, for each of the compounds, as a function of the incident proton energy. The nuclear reaction of interest is shown in (1):

$$^{226}\mathrm{Ra}\,(\mathrm{p},2\mathrm{n})\,^{225}\mathrm{Ac} \qquad (1)$$

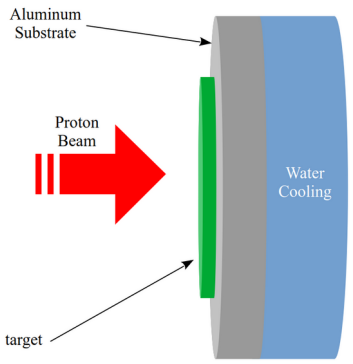

Figure 1: Geometry of targets containing ^{226}Ra compounds used in simulations to determine the optimal proton beam energy needed to produce the highest ^{225}Ac activity.

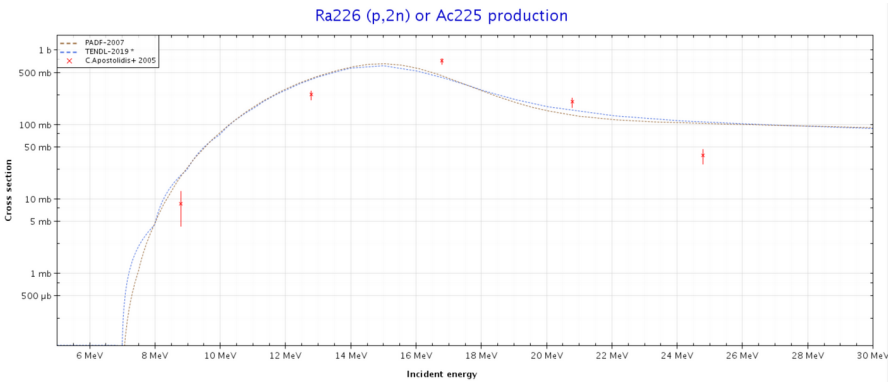

Figure 2: Cross-section as a function of energy for the nuclear reaction ^{226}Ra(p,2n)^{225}Ac.

The results obtained from these simulations showed that the best energy for activating ^{226}Ra and producing the highest ^{225}Ac activity is in the range between 14.6 and 15.3 MeV (hatched area in Figure 3).

The next step was to determine the appropriate geometries for each of the chosen targets, taking into account the density of each compound and the thermal conductivity. The thermal conductivity of each compound is quite different, ranging from 5 W/m.K to 19 W/m.K; therefore, the thicknesses of each target must be calculated individually for each compound. In any case, it is desired that the beam reaches 14.5 MeV of energy in some region of the target, so that the production of ^{225}Ac is as high as possible. Figure 4 shows the geometry used for these simulations: it consists of an aluminum beam collimator, 24 cm in diameter and 3 cm thick; The conical aperture of the collimator is 3 cm at the beam inlet and 1 cm at the beam outlet. The irradiation system itself consists of an energy degrader made of aluminum with a diameter of 1.6 cm and a thickness of 360 μm; a cooling channel with a diameter of 1.6 cm and a width of 0.5 cm; the target is surrounded by two silver foils with a diameter of 1.6 cm and a thickness of 30 μm; followed by another cooling channel identical to the first, and closing the entire system is a beam absorber made of aluminum with a diameter of 1.6 cm and a thickness of 1 cm. The thickness of the energy degrader was determined through simulations for a 30 MeV proton beam at the collimator inlet, so that, upon passing through the degrader, the first cooling channel, and the silver foil in front of the target, the beam energy is equal to 16 MeV upon reaching the target. Simulations were also performed for each of the ^{226}Ra compounds to determine the thicknesses so that, when passing through the target, the beam has an energy equal to 13 MeV. Figure 5 shows the energy spectra of the proton beam at three different positions for the case of the target made of metallic ^{226}Ra: before hitting the first silver window; before hitting the target; after passing through the target.

Based on these results, the masses of ^{226}Ra in each compound and their respective thicknesses were determined; these data are presented in Table I.

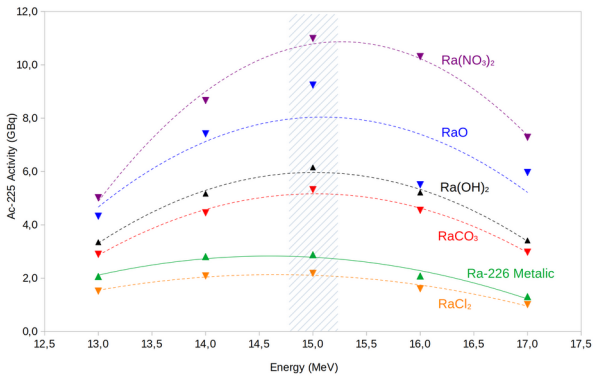

Figure 3: Activity of ^{225}Ac produced as a function of the energy of incident protons for each of the ^{226}Ra compounds studied.

Once the masses and thicknesses of the targets were determined, simulations were performed to determine the activities produced by ^{225}Ac in each case; the simulations also provided information on the beam energy loss as it passed through the irradiation system and on the thermal profile of the energy deposited throughout the system. All targets were irradiated for 45 h with a beam current of 50 μA. Figure 6 shows the dose curve and the thermal energy deposition profile for the ^{226}Ra target in metallic form; the curves and profiles for the other targets are similar.

The simulations presented here were performed on three personal computers: two with AMD Ryzen 5000 series 7 processors (8 cores/16 threads) and 64 GB of RAM, and one with a 14th-generation Intel Core i7 processor (4 cores/8 threads) and 64 GB of RAM. The applications used for the simulations were FLUKA 4-5.1 and FLAIR 3.4-5.2, both developed at CERN [14,15,16].

Table I. Characteristics of targets containing ^{226}Ra compounds for the production of ^{225}Ac.

Target	Mass of ^{226}Ra (mg)	Thickness (µm)	Target Density (g/cm^3)	Thermal Conductivity (W/m.K)
^{226}Ra Metalic	176,71	450	5.00	18.6
RaO	148,53	270	7.50	2.0 a 4.0
$Ra(OH)_2$	130,08	370	5.15	0.5 a 1.5
$RaCO_3$	112,95	350	5.20	1.5 a 2.5
$RaCl_2$	109,94	370	4.97	1.8 a 2.2
$Ra(NO_3)_2$	74,69	300	4.90	0.4 a 0.8

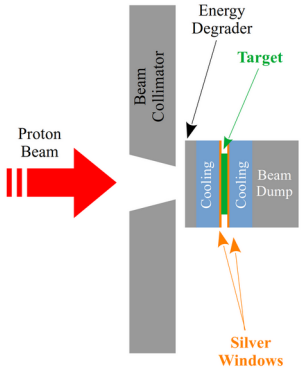

Figure 4: Geometry used to determine the thicknesses of each ^{226}Ra compound target.

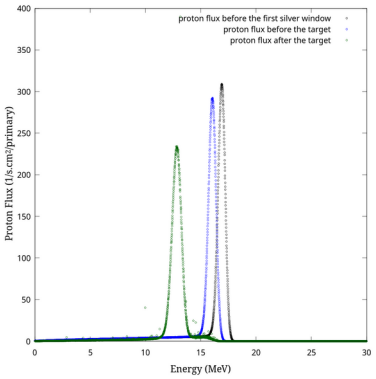

Figure 5: Energy spectra of the proton beam at three positions: before the first silver window; before the target; and after passing through the metallic ^{226}Ra target. For all other targets, the spectra are similar.

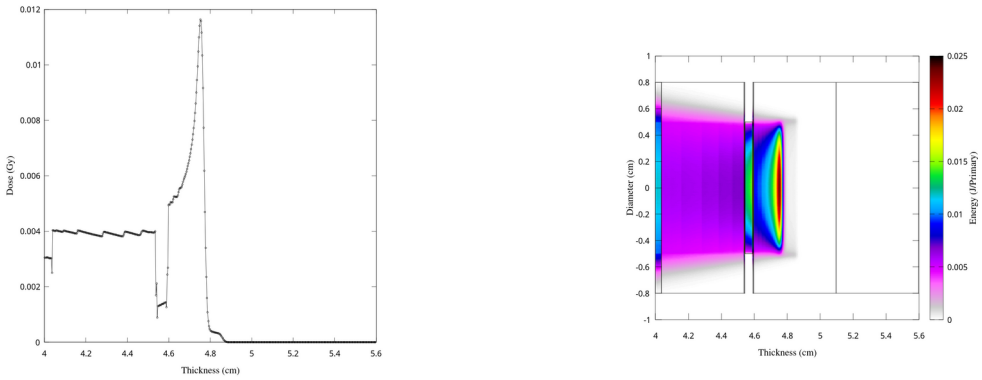

(a) **(b)**

Figure 6: **(a)** Energy loss throughout the irradiation system; **(b)** Thermal profile in the ^{226}Ra metallic target irradiated by a 16 MeV proton beam for 45 h with a beam current of 50 μA. For all other targets, the dose curve and energy deposition thermal profile are similar.

3. Results and Discussion

Table II presents the simulation results for the activities produced by ^{225}Ac during proton irradiation at four time points, for all ^{226}Ra compounds analyzed. The graph in Figure 7 shows the radioactive decay curves of ^{225}Ac. Since the masses of ^{226}Ra in each compound are different, an activity-by-mass graph (MBq/mg) was also created and is presented in Figure 8. In terms of practical yields, the values obtained at the end of irradiation (EOB) are presented in Table III.

Table II: Activities of ^{225}Ac produced in the irradiations of ^{226}Ra compounds at four different times.

Time (days)	**EOB**		**20**		**50**		**100**	
Target	**Activity (GBq)**	**ERR (%)**	**Activity (GBq)**	**ERR (%)**	**Activity (GBq)**	**ERR (%)**	**Activity (GBq)**	**ERR (%)**
Ra Metal	3.7752	0.3219	0.9448	0.3240	0.1184	0.3317	0.0038	0.3957
RaO	3.1946	1.239	0.7994	1.214	0.1002	1.154	0.0032	1.014
$Ra(OH)_2$	2.7689	0.4366	0.6928	0.4314	0.0868	0.4199	0.0027	0.4154
$RaCO_3$	2.3460	0.8155	0.5869	0.7999	0.0735	0.7654	0.0023	0.7558
$RaCl_2$	2.2608	0.6865	0.5654	0.7101	0.0707	0.7736	0.0022	1.047
$Ra(NO_3)_2$	1.6034	0.6316	0.4013	0.6336	0.0503	0.6422	0.0016	0.7253

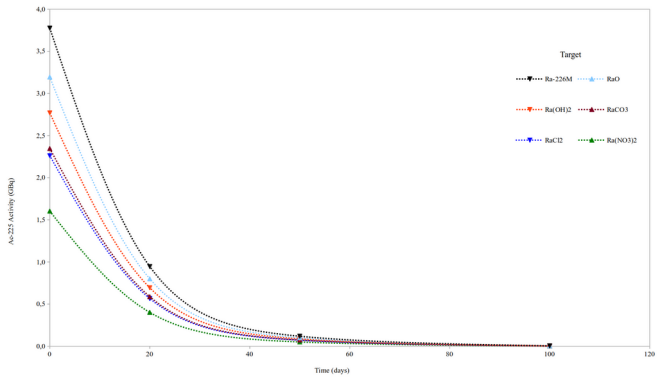

Figure 7: Radioactive decay of ^{225}Ac produced by irradiation of ^{226}Ra compounds.

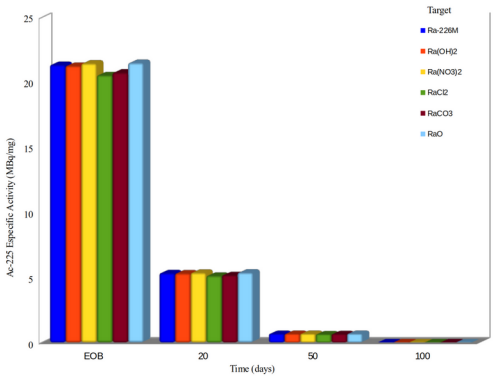

Figure 8: Specific activity of ^{225}Ac for each of the ^{226}Ra compounds studied.

Table III: Practical yields of ^{225}Ac produced in the irradiation of ^{226}Ra inorganic compounds.

Target	**Practical Yield**	
	(MBq/μAh)	**(μCi/μAh)**
Ra-226 Metalic	1.70	45.95
RaO	1.40	37.84
$Ra(OH)_2$	1.20	32.43
$RaCO_3$	1.04	28.11
$RaCl_2$	1.00	27.03
$Ra(NO_3)_2$	0.70	18.92

4. Conclusions

Although the geometries used for the simulations developed in this work are quite simple and do not account for all the experimental apparatus required for real proton-beam irradiation over long periods, the results show good agreement with values measured in experimental productions conducted in other countries [9,11]. The results obtained in the simulations made it clear that the best target for large-scale ^{225}Ac production is that made of purified ^{226}Ra in its metallic form; however, this type of target presents many technological complications, since the metallic material must be prepared in aqueous solution to allow electrodeposition on some inert metallic substrate, such as gold, for example. Electrodeposited targets present highly complex technical aspects both in preparation and in the subsequent dissolution and chemical separation of the target materials and products. The target, composed of Radium Oxide (RaO), also showed good practical yield; most oxides have high melting points, and the oxides of alkali

metals react strongly with water to form hydroxides, which are generally corrosive. The target, made of Radium Carbonate ($RaCO_3$), is a strong candidate for commercial production of ^{225}Ac because it can be easily obtained by reacting RaO with atmospheric carbon dioxide. In commercial terms, radium chloride ($RaCl_2$) is perhaps the most abundant and accessible, considering that most needles used in radiotherapy are composed of this type of salt. The radium nitrate ($Ra(NO_3)_2$) target is no less important than all the others, although it presented the lowest practical yield among all the targets analyzed in this work. On the other hand, this target has the lowest mass of ^{226}Ra among the others, which can be an advantage not only commercially but also from a practical standpoint when considering radiological protection issues in handling a target containing highly radioactive material.In the future, simulations of irradiation systems in cyclotrons will be improved to make them more realistic.

Acknowledgment

The authors of this work thank the Nuclear and Energy Research Institute (IPEN), especially the Center for Nuclear Engineering, for the opportunity to develop all the simulations in their facilities and for the use of the uninterruptible power supply (UPS) systems, which are of great importance when simulation times involve many hours or even days.

References

[1] KIM, YS., BRECHBIEL, M.W., An overview of targeted alpha therapy, Tumour Biol. 33 (2012) 573. 10.1007/s13277-011-0286-y
[2] TAFRESHI, NK., et al., Development of targeted alpha particle therapy for solid tumours, Molecules 24 (2019) 4314. 10.3390/molecules24234314
[3] MORGENSTERN, A., APOSTOLIDIS, C., BRUCHERTSEIFER F., Supply and clinical application of actinium-225 and bismuth-213, Semin Nucl Med. 50 (2020) 119. 10.1053 j.semnuclmed.2020.02.003
[4] RADCHENKO, V., et al., Production and supply of α-emitting radionuclides for targeted α-therapy, J Nucl Med. 62 (2021) 1495. 10.2967/jnumed.120.261016
[5] ROBERTSON, A.K.H., RAMOGIDA, C.F., SCHAFFER, P., RADCHENKO, V., Development of Ac-225 radiopharmaceuticals: TRIUMF Perspectives and Experiences, Curr Radiopharm. 11 (2018) 156. 10.2174/1874471011666180416161908
[7] MASTREN, T., et al., Simultaneous separation of actinium and radium isotopes from a proton irradiated thorium matrix, Sci Rep. 7 (2017) 8216.10.1021/acsomega.3c01769
[8] ROBERTSON, A.K.H., et al., 232Th spallation produced Ac-225 with reduced 227Ac content, Inorg Chem. 59 (2020) 12156. 10.1021/acs.inorgchem.0c01081
[9] C. APOSTOLIDIS, R. MOLINET, J. MCGINLEY, K. ABBAS, J. MÖLLENBECK, A. MORGENSTERN, Cyclotron production of Ac-225 for targeted alpha therapy, Applied Radiation and Isotopes 62 (2005) 383-387
[10] G. MELVILLEA,, H. MERIARTY, P METCALFE, T. KNITTEL, B.J. ALLEN, Production of Ac-225 for cancer therapy by photon-induced transmutation of Ra-226. Applied Radiations and Isotopes, 65 (2007) 1014-1022
[11] GRAEME MELVILLE, BARRY J ALLEN, Cyclotron and linac production of Ac-225, Applied Radiation and Isotopes 67 (2009) 549-555
[12] Kotaro Nagatsu, Hisashi Suzuki, Masami Fukada, Taku Ito, Jun Ichinose, Yoshio Honda, Katsuyuki Minegishi, Tatsuya Higashi and Ming-Rong Zhang, Cyclotron production of 225Ac from an electroplated 226Ra target, European Journal of Nuclear Medicine and Molecular Imaging, https://doi.org/10.1007/s00259-021-05460-7, (2021)
[13] https://cms.oecd-nea.org/janisweb/book/protons/Ra226/MT16/renderer/957

[14] C. Ahdida, D. Bozzato, D. Calzolari, F. Cerutti, N. Charitonidis, A. Cimmino, A. Coronetti, G. L. D'Alessandro, A. Donadon Servelle, L. S. Esposito, R. Froeschl, R. García Alía, A. Gerbershagen, S. Gilardoni, D. Horváth, G. Hugo, A. Infantino, V. Kouskoura, A. Lechner, B. Lefebvre, G. Lerner, M. Magistris, A. Manousos, G. Moryc, F. Ogallar Ruiz, F. Pozzi, D. Prelipcean, S.Roesler, R. Rossi, M. Sabaté Gilarte, F. Salvat Pujol, P. Schoofs, V. Stránský, C. Theis, A. Tsinganis, R. Versaci, V. Vlachoudis, A. Waets, M. Widorski, "New Capabilities of the FLUKA Multi-Purpose Code", Frontiers in Physics 9, 788253 (2022).
[15] André Donadon, Gabrielle Hugo, Christian Theis and Vasilis Vlachoudis *"FLAIR3 – recasting simulation experiences with the Advanced Interface for FLUKA and other Monte Carlo codes"* EPJ Web Conf. Volume 302, 2024 (SNA + MC 2024)
[16] V.Vlachoudis *"FLAIR: A Powerful But User Friendly Graphical Interface For FLUKA"* Proc. Int. Conf. on Mathematics, Computational Methods & Reactor Physics (M&C 2009), Saratoga Springs, New York, 2009